

PAPER

A dual natural lithium formate/L-alanine EPR dosimeter for a mixed radiation field in a boron neutron capture therapy irradiation facility

To cite this article: G Alejandro *et al* 2020 *J. Phys. D: Appl. Phys.* **53** 165001

View the [article online](#) for updates and enhancements.



IOP | ebooks™

Bringing you innovative digital publishing with leading voices to create your essential collection of books in STEM research.

Start exploring the collection - download the first chapter of every title for free.

A dual natural lithium formate/L-alanine EPR dosimeter for a mixed radiation field in a boron neutron capture therapy irradiation facility

G Alejandro^{1,2} , J Longhino^{1,3}, N R Álvarez¹, E Pawlak⁴ and A Butera^{1,2,3}

¹ Centro Atómico Bariloche—Comisión Nacional de Energía Atómica (CNEA), Av. E. Bustillo 9500, 8400 Bariloche, Río Negro, Argentina

² Consejo Nacional de Investigaciones Científicas y Técnicas (Conicet), Av. E. Bustillo 9500, 8400 Bariloche, Río Negro, Argentina

³ Instituto Balseiro (UNCuyo), Av. E. Bustillo 9500, 8400 Bariloche, Río Negro, Argentina

⁴ Centro Atómico Ezeiza—Comisión Nacional de Energía Atómica (CNEA), 1802 Ezeiza, Buenos Aires, Argentina

E-mail: galejand@cab.cnea.gov.ar (G Alejandro)

Received 8 October 2019, revised 23 December 2019

Accepted for publication 21 January 2020

Published 14 February 2020



CrossMark

Abstract

Standard commercial L-alanine pellets and specially prepared natural lithium formate monohydrate powder samples of specific granulometry were irradiated in a ⁶⁰Co gamma-ray irradiation plant and in the mixed field (thermal neutrons and gamma photons) of a boron neutron capture therapy (BNCT) experimental facility. The γ -doses applied with the ⁶⁰Co source range from 0.1 to 50 kGy, while those in the BNCT facility go from ~7 Gy to 150 Gy. The thermal neutron fluences range from 10^{12} neutrons cm^{-2} to 2×10^{13} neutrons cm^{-2} . The irradiation of materials promotes the creation of stable electronic defects (generally free radicals) which constitute paramagnetic centers that can be detected and quantified by electron paramagnetic resonance (EPR). After irradiation, the EPR characterization of the samples was performed by determining the EPR intensity of the spectrum relative to a reference standard constituted by Mn^{2+} impurities diluted into a MgO single crystal. As expected, L-alanine has revealed to be largely insensitive to thermal neutrons fluence in the investigated range. On the contrary, it is shown that the EPR intensity of irradiated natural lithium formate monohydrate powders is clearly sensitive to thermal neutrons and has a linear dependence with the γ -dose. We propose a dual dosimeter by combining L-alanine pellets and formate powders that would allow to determine the γ -dose and thermal neutron fluence in a selected position of the BNCT irradiation facility. Moreover, we demonstrate that the ⁶Li enrichment that has been proposed in the literature to enhance the performance of lithium-based EPR dosimeters is not crucial in our case. Instead, the natural isotopic abundance of lithium is large enough to obtain a satisfactory sensibility to thermal neutrons in our BNCT facility for fluences $>10^{12}$ neutrons cm^{-2} .

Keywords: electron paramagnetic resonance dosimetry, Lithium formate, L-alanine, mixed radiation fields, boron neutron capture therapy

(Some figures may appear in colour only in the online journal)

1. Introduction

Electron paramagnetic resonance (EPR, also named electron spin resonance-ESR) is a non-destructive technique which has been widely used to estimate doses of ionizing radiation in

multiple situations such as radiological emergencies [1, 2], medical therapies [3], industrial processes, dating of archaeological or paleontological samples, etc [4]. The principle of detection of EPR dosimeters consists on the ability of detecting and quantifying point paramagnetic defects, usually

free radicals, that are created by the ionizing radiation (photons, neutrons, electrons or other particles) incident on an adequate material. The intensity of the EPR signal is a reliable quantitative measure of the number of paramagnetic centers present in a sample. The EPR technique is non destructive and has been widely used to estimate doses in radiological emergencies, as well as in therapeutics and in industrial processes with ionizing radiation. Several materials can be used as EPR dosimeters, for example alanine [5, 6], hidroxyapatite (natural or synthesized), 2-methyl alanine, lithium formate, glucose, oxalates, phenols, etc [7–16]. The material of election depends on their dosimetric properties (sensitivity, time stability of the defects, linearity of the signal, etc) related to the specific application, and the dose interval of interest (ranging from some mGy to kGy). EPR dosimetry presents some advantages compared to other techniques, such as thermoluminescence, because of its non-destructiveness to read the dose and the sensitivity to doses in the kGy range.

One of the most popular compounds used today in EPR dosimetry is L-alanine [7]. On the one hand, it is widely used in industrial medium dose applications (50 Gy–10 kGy) such as blood or food irradiation (killing of parasites, slow ripening, etc) or high dose applications (10–50 kGy such as sterilization of food for immunocompromised people or to decontaminate some food additives, etc. On the other hand, the widespread use of alanine in low-dose (below 5 Gy) biomedical applications is due to its tissue equivalent properties, which minimizes the corrections in the determination of the received dose. Additionally, the free radicals responsible for the EPR spectrum (which consists on five lines as the product of the interaction of a single electron with four equivalent hydrogen nuclei) are very stable along time, and thus the signal remains practically unchanged even many years after the irradiation if the dosimeters are properly stored. Its response, which is reasonably linear in a wide range of doses, is independent of the dose rate [17] and the energy of the incident photon radiation [7]. The optimal range of dose detection for L-alanine commercial sensors is 10 Gy–100 kGy [7, 18]. Alanine is almost insensitive to thermal neutrons [19], and for this kind of radiation, doping with elements like boron or lithium, with a large neutron capture cross section and high LET products, are generally used to enhance the response [19–21].

Lithium formate monohydrate (abbreviated ‘LiFo’ in what follows) is an EPR dosimeter material that has some advantages in comparison with alanine [17, 22, 23]. LiFo’s atomic composition is closer to that of water what makes it more similar to organic tissues, has a higher sensitivity (5–6 times), presents a low energy dependence for clinical radiotherapy beams and has a simpler EPR, structureless spectrum than alanine’s, as it consists only on a single absorption line. Thus, LiFo dosimeters are a good alternative to alanine especially in the low dose range that is of concern in medical therapies [24].

In the last years LiFo has received considerable attention due to its ability to capture thermal neutrons through the nuclear reaction ${}^6\text{Li} + n \rightarrow {}^4\text{He} + {}^3\text{H}$ [25]. Indeed, the cross section for thermal neutrons capture of the ${}^6\text{Li}$ isotope (natural abundance 7.5%) is roughly $2 \cdot 10^4$ times larger than the majority isotope ${}^7\text{Li}$ [26]. Actually, the generation of

paramagnetic defects in lithium occurs indirectly through the capture of thermal neutrons by the minority ${}^6\text{Li}$ isotope, and the subsequent emission of alpha particles and tritium atoms which produce radiation damage in the material. Therefore, the irradiation of a LiFo dosimeter with thermal neutrons produces point paramagnetic defects in the material that could be detected and quantified by electron spin resonance [26]. This is especially relevant for applications in medical therapies that make use of mixed radiation fields of photons and thermal neutrons.

A relevant case is boron neutron capture therapy (BNCT), where the characterization of the radiation field in a certain position of the facility, that implies the simultaneous determination of the photon dose and the thermal neutron fluence, is crucial to manage the appropriate settings for the BNCT therapy [27–29]. Most efforts have been focused on studying the EPR dosimetric properties of ${}^6\text{Li}$ -enriched LiFo due to its better sensitivity and its ability to detect thermal neutrons. A dual dosimeter that would combine the simultaneous EPR readings of both natural Li and ${}^6\text{Li}$ -enriched LiFo pellets has been proposed in the past to characterize a mixed field of gamma photons and neutrons [26]. In this paper we explore the possibility of designing a LiFo-based dosimeter with no need of ${}^6\text{Li}$ isotopic enrichment. In particular, we propose a combined L-alanine/natural LiFo EPR dosimeter capable to achieve a satisfactory performance in the mixed field of a particular BNCT facility.

2. Materials and methods

2.1. Preparation of the samples

The samples used in this work were prepared from commercial lithium formate monohydrate ($\text{LiCOOH} \cdot \text{H}_2\text{O}$ 98%, Sigma Aldrich) powders. The first step of the route of preparation consisted on the grinding of the initial powder in a ball-mill rotating at an average speed of 50 rpm. The progress of the milling was checked by observing the powders from time to time using a stereomicroscope. The total time of milling was roughly one hour. In figure 1 we can observe the progressive diminishing of the particle size of the lithium formate monohydrate powder by comparing pictures corresponding to milling times of 7 min (left) and 42 min (right). A rough estimation from the micrographs gives that the average particle size was reduced from more than $300 \mu\text{m}$ to less than $200 \mu\text{m}$.

The milling process contributes to the efficiency of the next step of the preparation, which is the sieving. The main purpose of performing a sieving after the milling process was to guarantee the reproducibility of the particle size distribution across the whole sample series in order to be able to make secure comparisons between samples, eliminating an extra source of uncertainty. After milling, the powders were sieved at 1000 rpm in a vibrating tower of five sieves with stainless steel mesh, piled over a collecting tray at the bottom. The micrometric nominal size of the mesh diminished from top to bottom: $177 \mu\text{m}$, $105 \mu\text{m}$, $74 \mu\text{m}$, $37 \mu\text{m}$ and $25 \mu\text{m}$, respectively. We noted that the sieving becomes more efficient when some balls from the mill are introduced into the sieves. The

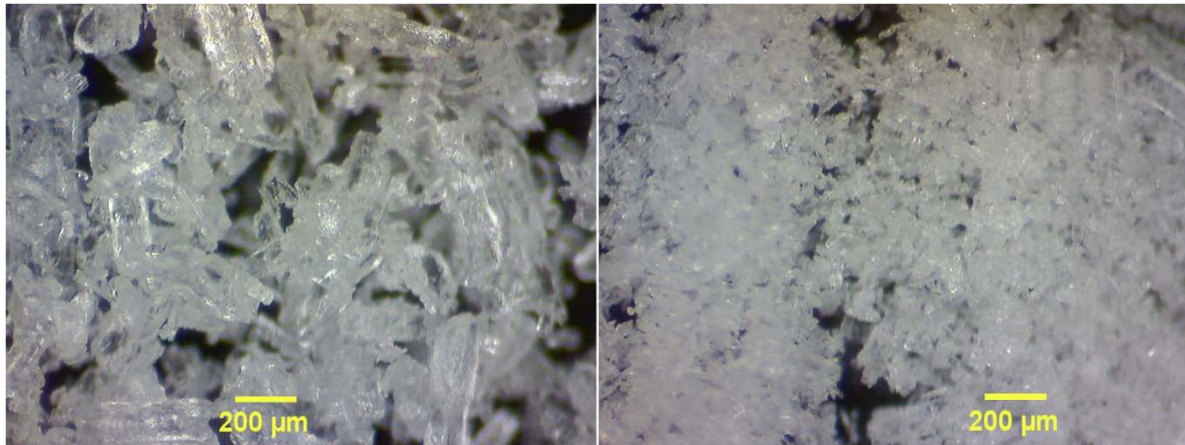


Figure 1. Stereomicroscope pictures of LiFo powder captured during the milling process: 7 min (left) and 42 min (right).

sieving finishes when after some time we observe that there is no more accumulation of powder in the collecting tray. To perform the irradiation experiments we decided to work with the powder remaining in the $37\ \mu\text{m}$ sieve, i. e. the nominal particle size of the selected powder ranges from $37\ \mu\text{m}$ to $74\ \mu\text{m}$.

2.2. Irradiation protocols

2.2.1. Gamma photons irradiation. Harwell Radspin commercial EPR dosimeters [18, 30], widely used in routine industrial and semi industrial irradiations, were irradiated in the ^{60}Co gamma-ray source with an activity of approximately $2.2 \cdot 10^4$ TBq (600kCi) at PISI (Planta de Irradiación Semi-Industrial) in Centro Atómico Ezeiza, Buenos Aires, Argentina. Irradiation doses at PISI are traceable to National Physical Laboratory (NPL-UK) standards through the irradiation of L-alanine pellets at known doses in the range 20 Gy–80 kGy. The combined uncertainty in the local irradiation of alanine pellets is estimated in 1.7% (considering the NPL irradiation uncertainty, the variations in different dosimeters irradiated to the same dose, variations in mass and the uncertainty in the calibration curve). We applied γ -doses ranging from 0.1 kGy to 50 kGy. The dose rates selected to perform the irradiations were $17\ \text{kGy h}^{-1}$ for doses equal to and higher than 4 kGy, $6\ \text{kGy h}^{-1}$ for 1 kGy, and $21\ \text{Gy min}^{-1}$ for 0.1 kGy, at sample distances of 0.3 m, 0.8 m, and 2.2 m from the center of the source, respectively. The pellets, composed of 90.9% (weight) L-alanine and 9.1% (weight) paraffin wax as binding agent, are cylindrical with slanted edges, and have a diameter of 5 mm and a height of 2.2 mm. A control sample of LiFo powder in a plastic Eppendorf tube was also irradiated at the lowest available (113 Gy) γ -dose.

2.2.2. Mixed field (gamma photons + thermal neutrons) irradiation. The irradiations in a mixed field of gamma photons and neutrons were carried out at the BNCT facility of the experimental reactor RA6 (Centro Atómico Bariloche, Rio Negro, Argentina). A set of standard L-alanine Harwell commercial dosimeters and our powder samples of lithium formate monohydrate were irradiated simultaneously at the same radiation source. The irradiations performed in the mixed field

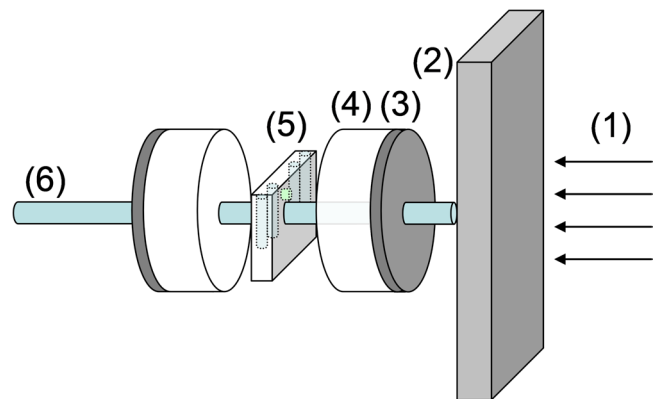


Figure 2. Scheme of the BNCT irradiation set-up. (1) Incoming mixed neutron–photon radiation from the reactor. (2) Bismuth shield (65 cm diameter) to reduce the gamma photon component of the radiation. (3) Removable cadmium disc (diameter: 12 cm, thickness: 0.8 mm) for the absorption of thermal neutrons. It is positioned 2 cm apart from the bismuth shield. The other cadmium disc is permanently fixed. (4) Polyethylene disc (diameter: 12 cm, thickness: 25 mm) for the thermalization of neutrons. (5) Sample holder ($10\ \text{cm} \times 5\ \text{cm} \times 1.9\ \text{cm}$), in direct contact with the polyethylene discs (not to scale in the drawing). It can hold four quartz tubes and an alanine monitor at the center. (6) Aluminum rod to hold the discs and the sample holder.

of the BNCT source were characterized by neutron fluences of the order of $10^{12}\ \text{n cm}^{-2}$ (with neutron fluxes in the range $3.7\text{--}12.810^8\ \text{n cm}^{-2}\ \text{s}^{-1}$) whereas the values of γ -doses range roughly between 7 Gy and 150 Gy. In figure 2 we show a schematic drawing of the BNCT experimental setup.

The radiant fields were obtained by increasing neutron thermalization and photon production from an originally unperturbed mixed field in a selected position into the BNCT external collimator. As the BNCT beam was originally designed with a strong epithermal neutrons component, further neutron moderation was required to increase the thermal neutron flux intensity while diminishing fast and epithermal flux, thus providing a more developed moderation-thermalization neutron spectrum. The increment in neutron thermalization was performed by a frontal polyethylene plate (see figure 2) with enough thickness (25 mm) to produce a thermalization peak wide enough to assure high flux in selected

Table 1. Neutron fluences and γ -dose values corresponding to irradiation of Harwell L-alanine pellets and LiFo powders in three different configurations: two at BNCT (mixed radiation field) and one at PISI (gamma photons source). The maximum relative uncertainties of neutron fluences are approximately 6%, while those of γ -doses are lower than 5% and 6% for L-alanine pellets and LiFo powders, respectively.

Configuration of irradiation	Irradiation time (min)	Neutron fluence (L-alanine pellets) (10^{12} n cm^{-2})	γ -dose (L-alanine pellets) (Gy)	Neutron fluence (LiFo powder) (10^{12} n cm^{-2})	γ -dose (LiFo powder) (Gy)
#1 (BNCT)	140	4.0	145.0	3.0	135.0
	105	3.0	109.0	2.3	101.0
	84	2.4	87.0	2.0	81.0
	52	1.6	54.0	1.3	50.0
	8	0.23	8.5	0.18	7.9
#2 (BNCT)	340	26.0	115.0	19.0	159.0
	220	17.0	—	12.0	103.0
	120	9.0	—	6.8	56.0
#3 (PISI)	5.5	—	—	0.0	113.0

off-axis positions (in which the samples are placed). A similar plate was placed behind the sample holder to provide a favorable neutron diffusion boundary. The sample holder was also made from a neutron moderator as to complement the characteristics of the moderator plates. With this experimental setup the thermal flux to epithermal constant ratio ≈ 33 , as determined by the preliminary experimental model validation using several AuCu activation detectors. We can also notice that such flux distribution will produce ${}^6\text{Li}$ (n, α) ${}^3\text{H}$ reactions with more than 95% of them being produced with thermal captures (neutron energies below 0.5 eV), as obtained through MCNP calculation, and can also be confirmed from usual 2-group activation calculations.

The most important contributions to the gamma photons spectrum are defined by the spectral components at characteristic energies arising from thermal neutron capture in hydrogen (2.2 MeV) and cadmium (remarkably 558 and 651 keV, plus others with lower probability), and finally the broad peak arising from the prompt photon energy distribution from fission events, prompt captures, and the fission products decay as they are generated into the core and pass through the several filtering stages of the BNCT beam setup. To increase the photon dose (i.e. in configuration #1), an extra 0.8 mm thick metallic cadmium plate is added ahead the frontal moderator (the other cadmium plate behind the rear neutron reflector remains fixed). The cadmium plates increase the total gamma photon production via the prompt thermal neutron absorption reaction ${}^{113}\text{Cd} + n \rightarrow {}^{114}\text{Cd} + \gamma$ at the boundaries of the holder/moderator array. This will also produce a moderated reduction of the holder's thermal neutron flux due to overall change in boundary conditions.

In order to minimize the sample neutron self shielding and homogenize the radiation fields, the LiFo powders were irradiated in 4 mm diameter quartz tubes of EPR quality cut to a length of 6 cm. An ad hoc setup was devised to place all the samples (L-alanine pellets and LiFo tubes) into the irradiation area. It was composed of a thin rectangular holder, properly drilled to fit three symmetrically disposed tubes, and one tube containing a flux monitor, as well as a symmetrically centered Harwell L-alanine dosimeter.

The thermal neutron fluence for each individual sample was derived from the measurement of an AuCu activation detector at the flux monitor position. That experimental value was then extended to the samples by using scaling factors derived from a criticality calculation on the detailed modeling of the geometry—RA6 core (BNCT facility) and experimental device (including holder, moderators, cadmium plates, sample tubes, etc)—using the Monte Carlo code MCNP5 [31]. The calculated scaling factors for neutron fluxes were previously validated in an experimental setup of the holder without the EPR-based detectors, replacing them with AuCu neutron activation detectors.

Similar procedures were performed for the individualization of the calculated photon doses in samples [32], using TLD-700 as the γ -dose monitors in a previous photon scaling factor validation procedure. The summary of the irradiation parameters are given in table 1. The data of a LiFo powder sample irradiated at the PISI (${}^{60}\text{Co}$ source) is also included.

After irradiations, and by performing the EPR characterization (see next section) of the L-alanine Harwell pellets irradiated at the PISI (used as dose standards) and BNCT facilities, we obtained EPR-derived γ -doses, which were found to be larger ($\approx 40\%$) than those determined from the TLD monitors. This discrepancy may obey to several reasons. One of them is the fact that the TLD monitors were not operating in its optimal (i.e. linear) range at BNCT. Actually, this value is consistent with the results reported in [33], where important saturation effects of TLD are reported for doses above 5 Gy. Other reason for discrepancy is that the specific characteristics of the irradiation setups used in both facilities are different. However, from the data presented in the next section we can discard an additional EPR signal in the alanine pellets due to the influence of the thermal neutrons. For the purpose of this work we decided to renormalize the γ -doses read from the TLD dosimeters to values consistent with our EPR calibration by just applying a scaling factor. Regarding the γ -doses received by the LiFo powders (irradiated in quartz tubes), it is enough to use a proportionality factor between pellets and tubes that it is determined by the specific geometry of our irradiation setup.

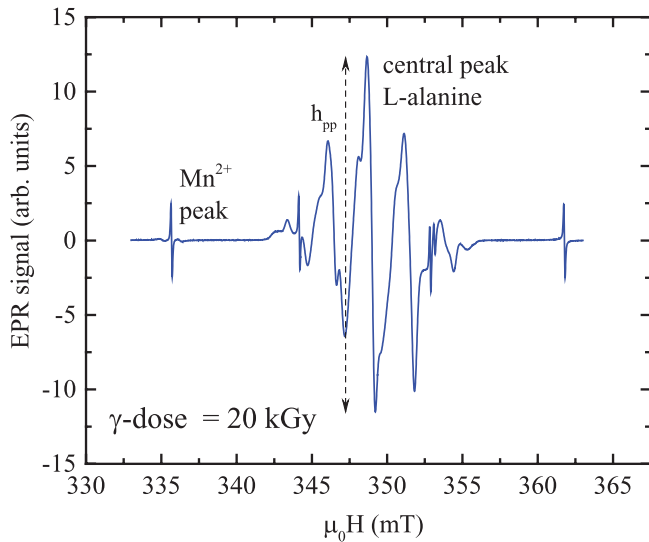


Figure 3. Room temperature L-alanine EPR spectrum (microwave frequency of 9.7 GHz) measured on a Harwell commercial pellet irradiated with a γ -dose of 20 kGy. The peaks of the Mn^{2+} standard reference are also shown. The peak-to-peak height (h_{pp}) of the central L-alanine and the Mn^{2+} peaks are used to calculate the EPR intensity (referred to the Mn^{2+} standard).

2.3. EPR characterization of irradiated samples

The post-irradiation EPR experiments were performed at room temperature at a microwave frequency of 9.7 GHz (X band) and 0.63 mW power using a standard rectangular, ultra-clean TE 102 microwave cavity in a Bruker ELEXSYS E500 spectrometer. The first derivative of the absorbed microwave power, which is commonly used to plot the EPR spectrum, was detected by modulating the static magnetic field with an AC field of 100kHz and amplitude of 0.05 mT. This value was chosen to avoid the overmodulation of the Mn^{2+} reference signal (see next section) that has an intrinsic linewidth of ~ 0.1 mT. To ensure the linear response of the resonant physical system it is also important to work under non-saturating conditions, particularly for the Mn^{2+} reference signal. This is assured by using a low microwave power of 0.63 mW.

3. Results

3.1. EPR characterization of L-alanine pellets irradiated with gamma photons

The combined EPR spectrum of L-alanine Harwell pellets and a $\text{MgO}:\text{Mn}^{2+}$ single crystal used as a reference standard is shown in figure 3. Actually, diluted Mn^{2+} paramagnetic ions, with $S = 5/2$ and $I = 5/2$ have been widely used as reference signals in quantitative EPR analysis [4–6, 9]. They show a sextet of equally spaced (by ~ 9 mT) lines due to the hyperfine coupling between electronic and nuclear spins. The L-alanine spectrum consists of five lines arising from the interaction of a single electron with four nearby equivalent protons. Actually, what we determine from the spectra is the ratio between the peak-to-peak height (h_{pp}) of the central peak of L-alanine and h_{pp} of one peak of the Mn^{2+} reference (see

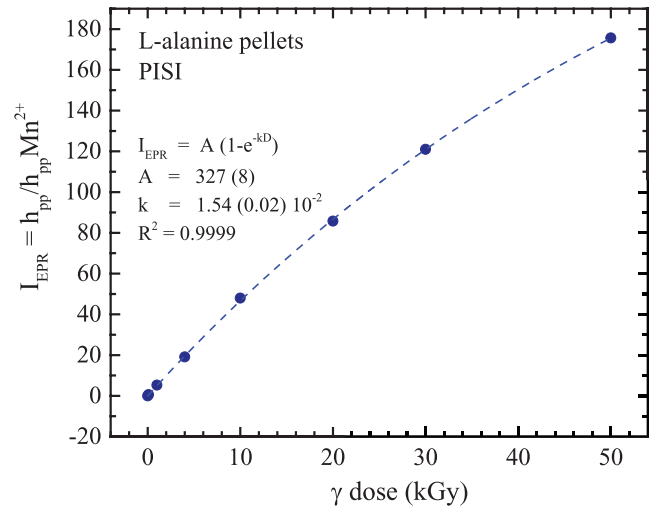


Figure 4. EPR intensity (relative to Mn^{2+} standard) measured on L-alanine Harwell pellets irradiated in the gamma photon flux of the Gammacell source at PISI. The vertical error bar is smaller than symbol size. Inset: zoom of the range 0–1000 Gy, where a pellet irradiated at the mixed field of the BNCT facility (γ -dose ≈ 100 Gy) is inserted for comparison. The maximum relative uncertainty in the determination of the γ -dose is 5% for doses < 100 Gy and proportionally smaller for higher doses.

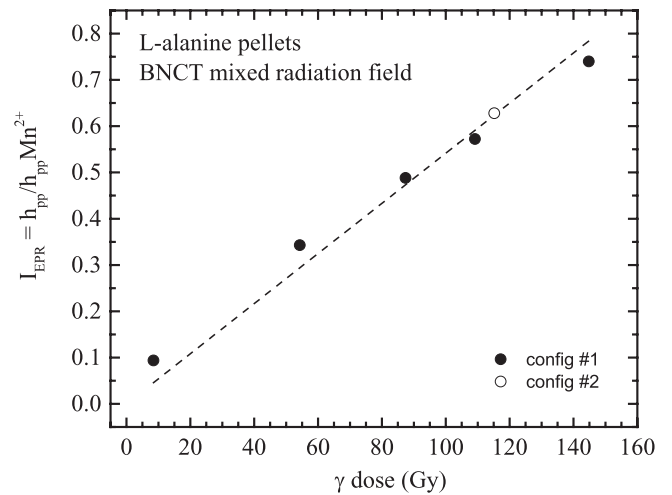


Figure 5. EPR intensity measured on Harwell L-alanine pellets (relative to the Mn^{2+} standard) irradiated in the mixed radiation field of the BNCT facility as a function of the γ -dose reported in table 1. The experimental errors in I_{EPR} are smaller than the symbol size. The dashed line is the linear approximation, valid for doses lower than 1 kGy ($R^2 = 0.974$). The maximum relative uncertainty in the determination of the γ -dose is 6%.

figure 3). The $\text{MgO}:\text{Mn}^{2+}$ crystal used as reference is fixed to a sample holder specially designed to simultaneously hold the reference and center the quartz tube employed to contain the powder (or pellet) sample. The use of the centering sample holder guarantees that the position of the samples inside the microwave cavity remains unchanged throughout the whole series of measurements, thus minimizing the experimental uncertainties.

With this procedure, both the L-alanine pellet and the Mn^{2+} reference are measured simultaneously during the same scan,

Table 2. Number of averaged scans used to collect the EPR spectrum of the different samples.

L-alanine pellets BNCT (γ -dose in Gy)	LiFo powder BNCT (γ -dose in Gy)	LiFo powder (PISI) (γ -dose in Gy)	Number of averaged scans
145.0			10
109.0			15
87.0			15
54.0			30
8.5			58
	159.0		10
	103.0		15
	56.0		15
		113 Gy	25

ensuring that the determination of the EPR intensity is independent from eventual instrumental fluctuations that occur from one scan to another. By calculating the ratio of EPR intensities of L-alanine and Mn^{2+} reference we obtained a calibration function I_{EPR} versus γ -dose in the range 0–50 kGy, as shown in figure 4. All the EPR spectra used to plot figure 4 were collected by averaging 5 scans, except for sample with the lower dose (0.1 kGy), for which 10 scans were averaged to improve the signal-to-noise ratio.

As recommended by the manufacturer of the alanine pellets, the EPR line intensity (I) versus dose (D) can be well described by an exponential dependence $I_{\text{EPR}} = A(1 - e^{-kD})$, where A and k are fitting constants. A gives the asymptotic value of I_{EPR} for ‘infinite dose’ and k , which determines the curvature of the function, has units of kGy^{-1} . The quality of the fitting is excellent, as expressed by the correlation coefficient $R^2 = 0.9999$. However, for doses below 1 kGy, the exponential term can be well approximated by a linear function, giving an EPR intensity that is proportional to the radiation dose (see inset of figure 4). Please note that for determining the γ -doses received by L-alanine pellets irradiated at the BNCT facility, which are of the order of (or smaller than) 100 Gy, we used the low-dose, linear function shown in the inset.

3.2. EPR characterization of L-alanine pellets and LiFo powders irradiated in a mixed radiation field

As our goal is to accurately determine the intensity of the EPR response we tried to avoid making ulterior corrections induced by differences in the filling factor of the microwave cavity. For this reason we filled all the EPR tubes with a fixed amount of 120 mg (with a dispersion of 1%) of irradiated LiFo powder to keep the cavity filling factor constant and operating in a condition for which the detected EPR signal is independent of the sample mass. In this way we were able to safely read the measured intensity without normalizing by sample mass, filling factor, or perform other kind of corrections. In table 2 we indicate the number of averaged scans used to collect the EPR spectrum of each sample considered in this section.

In figure 5 we plot the ratio $I_{\text{EPR}} = h_{pp}^{L-al} / h_{pp}^{\text{Mn}^{2+}}$ as a function of the γ -dose absorbed by commercial Harwell L-alanine pellets during irradiations performed at the BNCT facility. As expected, we observe that in this dose range there is a clear linear dependence of the EPR intensity on the γ -dose.

From figure 5 we observe that there is a single linear dependence of the EPR signal on γ -dose, regardless of the value of neutron fluence (see table 1). At first glance it seems that the proposed fitting is not the best achievable. It should be noted that the linear fit was done using only one adjustable parameter, i.e. the slope. Indeed, the ordinate is fixed at 0 to satisfy the condition $I_{\text{EPR}}(\gamma\text{-dose} = 0) = 0$. It must be guaranteed that there are not free radicals in the samples previous to the beginning of the irradiation and thus the EPR intensity must vanish at zero dose. This constraint explains the fact that the linear fit in figure 4 is best possible one with just only one adjustable parameter. However, the linear relationship between absorbed dose and I_{EPR} is clear and unambiguous. Therefore, L-alanine has revealed to be largely insensitive to thermal neutrons fluence in the investigated range, as expected from previous literature [19] and already mentioned in the previous section.

In figure 6 we show the EPR spectra of LiFo powders (measured into quartz tubes) irradiated in the three irradiation configurations summarized in table 1 with γ -doses close to 100 Gy.

The LiFo EPR spectrum consists on a single line having a width of 1.4 mT. It was demonstrated that the dominant radical species produced after irradiation, and consequently the main responsible for the EPR absorption is a CO_2^- radical [34, 35]. The hyperfine coupling of this unpaired electron with the Li nuclei is not resolved, but it has been shown that ^6Li -enriched LiFo presents a narrower line than natural LiFo due to the lower nuclear spin and smaller hyperfine coupling constant of ^6Li compared to the more abundant (92.5%) ^7Li isotope [26]. It is evident that the EPR intensity varies significantly in the three cases: while it is minimum for the sample that received no neutron flux (config. #3), it is maximum in the case of maximum thermal neutrons fluence (config. #2). Therefore, at variance with L-alanine, the EPR intensity of irradiated LiFo powders is clearly sensitive to thermal neutrons. This can be observed in figure 7, that shows I_{EPR} versus γ -dose for LiFo powder samples irradiated in the mixed field of the BNCT facility.

In this case we immediately note that the experimental points are grouped into two sets with linear behavior, corresponding to the two different irradiation configurations detailed in table 1. We note that in this case, the vanishing condition $I_{\text{EPR}}(\gamma\text{-dose} = 0) = 0$ that constraints the fitting of

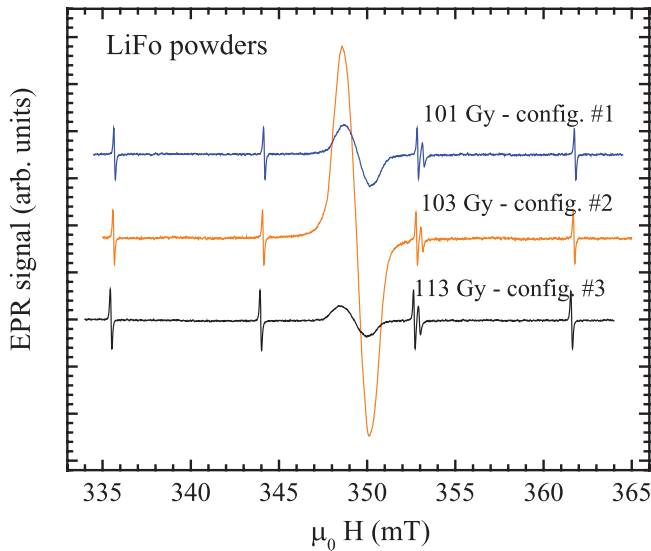


Figure 6. Room temperature EPR spectra of LiFo powders irradiated with γ -doses close to 100 Gy in the different configurations of table 1 (config. #1 and config. #2: BNCT, config. #3: PISI). The peaks of the Mn^{2+} standard reference spectrum are also shown.

the experimental data also applies (see the above explanation given for figure 5). In configuration #2 the thermal neutron fluencies are higher than in configuration #1, while the values of gamma dose span roughly the same range. It becomes evident that the EPR intensity is a sensitive parameter capable to discriminate well between samples irradiated with similar gamma doses but with different neutron fluencies. It is remarkable that the ability to efficiently detect thermal neutrons was achieved using natural lithium formate monohydrate powders instead of the usually invoked 6Li -enriched compound, which makes this kind of powder an excellent and relatively inexpensive material to be used as a sensor for a mixed radiation field.

4. Model

We will now consider the above experimental results in terms of a radiation sensor operating in a mixed radiation field of gamma photons and thermal neutrons.

Let us define y as the measured EPR intensity (I_{EPR}) which is proportional to the of paramagnetic defects created in the material as a consequence of irradiation in a mixed field of gamma photons and thermal neutrons. Consider y_γ and y_n as the partial contributions to the total number of electronic defects produced by gamma photons and thermal neutrons radiation, respectively. Then:

$$y = y_\gamma + y_n = \gamma x_\gamma + n x_n, \quad (1)$$

where x_γ and x_n are the γ -dose and thermal neutrons fluence respectively, and γ and n are constants that depend exclusively on the specific irradiated material. In the two terms of the above equation we have assumed that the number of radiation-induced defects is linearly proportional to the γ -dose and the neutron fluence, which is expected to hold in the studied range of gamma photon doses and neutron energies. The constants

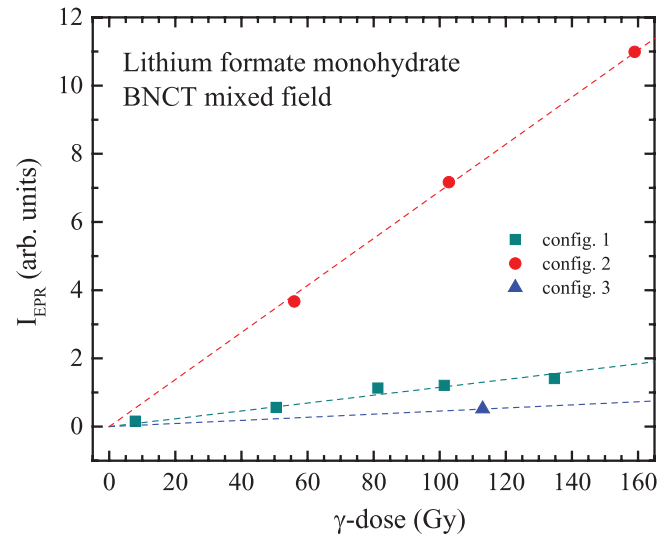


Figure 7. EPR intensity measured on LiFo powders (relative to the Mn^{2+} standard) irradiated at the mixed radiation field of the BNCT facility (configurations #1 and #2). The triangle symbol corresponds to a powder LiFo sample irradiated with gamma photons at the PISI (see table 1). The dashed lines are the linear fittings from which we obtained the constants B_j ($j = 1-2$). The correlation coefficients are $R^2 = 0.94$ for config #1 and $R^2 = 0.998$ for config #2, respectively. The line for configuration #3 is the straight line passing through the experimental point (triangle) and the origin of coordinates. The maximum relative uncertainty in the determination of the γ -dose is 6%.

γ and n in equation (1) actually define our mixed-field sensor in a way that, once they are fixed, equation (1) can be used to determine the γ -dose and neutron fluence for a wide range of unknown irradiation configurations (i.e. an unknown selection of γ -dose and neutron fluence). Therefore, the goal is to calculate γ and n from the above EPR results.

If $j = 1, 2, \dots, N$ is the index that enumerates N different irradiation configurations, we can define the ratios

$$A_j \equiv x_n(j)/x_\gamma(j) \quad (j = 1, \dots, N). \quad (2)$$

Then we can express equation (1) in terms of the γ -dose only:

$$y_j = (nA_j + \gamma) x_\gamma = B_j x_\gamma(j). \quad (3)$$

Note that a linear fit of equation (2) allows to determine A_j ($j = 1, \dots, N$) as the slope of the plot $x_n(j)$ versus $x_\gamma(j)$, being the fluences ($x_n(j)$) and the γ -doses ($x_\gamma(j)$) the experimental parameters defining the N irradiations. Similarly, a linear fit of the measured EPR intensities (y_j) and the γ -doses (equation (3)) allows to determine B_j ($j = 1, \dots, N$), as shown in figure 7. Note that for irradiations carried out with the ^{60}Co gamma source at PISI, $A_j \equiv 0$ as there is no neutron flux. In table 3 we summarize the values of (A_j , B_j) determined for three configurations of irradiation ($N = 3$) of LiFo powders:

According to equation (3), there is a linear relation connecting A_j and B_j :

$$nA_j + \gamma = B_j.$$

Then, using the three configurations in table 3 and performing a linear regression $B_j(A_j)$, we obtain n and γ from the slope and the ordinate, respectively:

Table 3. A_j and B_j as obtained from the linear regressions defined by equations (2) and (3). We omitted units for simplicity: A_j are expressed in 10^{12} neutrons $\text{Gy}^{-1} \text{cm}^{-2}$ and B_j in terms of Gy^{-1} . The values in parenthesis are the output errors of the linear regressions from which A_j and B_j were derived.

Configuration #1 (BNCT)	$A_1 = 0.0234$ (5)	$B_1 = 0.0115$ (6)
Configuration #2 (BNCT)	$A_2 = 0.12144$ (7)	$B_2 = 0.0690$ (7)
Configuration #3 (PISI)	$A_3 = 0$	$B_3 = 0.0045$

$$n = (0.55 \pm 0.05) 10^{-12} \text{ cm}^2/\text{neutrons}$$

$$\gamma = 0.002 \pm 0.003 \text{ Gy}^{-1}.$$

We immediately note that while the error in the determination of n is below 10%, the uncertainty in γ is more that 100%. Actually, the uncertainty in γ arises from the very high sensibility of LiFo to thermal neutrons, which prevents from determining with enough precision the relatively small signal originating in the gamma-induced paramagnetic centers. This implies that for the chosen combination of neutron fluences and γ -doses the gamma term in equation (1) will not be accurately determined to characterize the mixed field. The determination of γ could be significantly improved by increasing the number of points of the linear regression B_j (A_j), i.e. by increasing the number of configurations of irradiation employed to determine n and γ . This solution, though feasible, is very time consuming (see table 1) and therefore depends strongly on the schedule availability of the irradiation facility. Nevertheless, the proposed method to be followed is straightforward.

5. Conclusions

In this work we presented a protocol for the irradiation of samples of commercial L-alanine pellets and specially prepared powders of natural lithium formate monohydrate in the mixed field of gamma rays and thermal neutrons of a BNCT facility. Complementary irradiations performed with a ^{60}Co gamma rays source were also added. The irradiations were followed in all cases by the careful measurement of the EPR spectrum produced by the electronic defects induced in each sample by the ionizing radiation. We showed that while the EPR intensity measured on L-alanine is linear with the γ -dose and seems to be rather insensitive to the irradiation with thermal neutrons, lithium formate monohydrate powders exhibit a strong dependence of the EPR intensity with neutron fluence.

Based on the EPR results obtained from three different configurations of the BNCT mixed field at a fixed position, and extra data from irradiations with the ^{60}Co gamma ray source, we propose a model where the determination of the main parameters γ and n would allow to estimate unknown values of γ -dose and neutron fluence in another position of interest in the BNCT facility.

Therefore, when the constants γ and n are determined, we can get a dual sensor to be used in the mixed field of gamma

photons and thermal neutrons. This sensor would consist on an L-alanine pellet and a powder sample of LiFo that would allow to determine the γ -dose and thermal neutron fluence in a selected position of the irradiation facility. The reading of the EPR intensity measured on the L-alanine pellet gives straightforwardly the γ -dose by comparison with the gamma photon calibration performed at the PISI (with the ^{60}Co gamma ray source, see figure 4). Instead, the EPR intensity measured on the LiFo sample allows to calculate the unknown thermal neutron fluence from equation (1) using γ , n and the γ -dose as inputs. We note that for high values of neutron fluencies, the EPR intensity allows to determine the neutron fluence directly, with little influence of the gamma photon contribution, which is much smaller.

At variance with other dosimeters discussed in the literature [22, 26], our proposed sensor does not require ^6Li -enriched lithium formate monohydrate. Actually, we have demonstrated that the natural isotopic abundance of lithium is good enough to obtain a satisfactory sensibility to thermal neutrons in our BNCT facility for fluences in the range of 10^{12} – 10^{13} n cm^{-2} .

Acknowledgments

This work was partially supported by Conicet under Grant PIP 201501-00213, ANPCyT Grant PICT 2013-040 and UN Cuyo Grant 06/C484. The technical support from Rubén E Benavides, César Pérez and Matías Guillén is deeply acknowledged.

ORCID iDs

G Alejandro  <https://orcid.org/0000-0002-1510-107X>

References

- [1] Sproull M and Camphausen K 2016 *Radiat. Res.* **186** 423–35
- [2] Bailiff I K, Sholom S and McKeever S W S 2016 *Radiat. Meas.* **94** 83–139
- [3] Marrale M, Carlino A, Gallo S, Longo A, Panzeca S, Bolsi A, Hrbacek J and Lomax T 2016 *Nucl. Instrum. Methods Phys. Res. B* **368** 96–102
- [4] Lund A and Shiotani M 2014 *Applications of EPR in Radiation Research* (Berlin: Springer)
- [5] Baffa O and Kinoshita A 2014 *Radiat. Environ. Bioph.* **53** 233–40
- [6] Baffa O, Kinoshita A, Abrego F C, dos Santos A B, Rossi B and Graeff C 2004 *AIP Conf Proc.* **724** 41
- [7] Regulla D F and Deffner U 1982 *Int. J. Appl. Radiat. Isot.* **33** 1101–14
- [8] Lund A, Olsson S, Bonora M, Lund E and Gustafsson H 2002 *Spectrochim. Acta A* **58** 1301–11
- [9] Borgonove A F, Kinoshita A, Chen F, Nicolucci P and Baffa O 2007 *Radiat. Meas.* **42** 1227–32
- [10] Fattibene P and Callens F 2010 *Appl. Radiat. Isot.* **68** 2033–116
- [11] Antonovic L, Gustafsson H, Carlsson G A and Tedgren Å C 2009 *Med. Phys.* **36** 2236
- [12] Korkmaz G, Dilaver M and Polat M 2019 *Appl. Radiat. Isot.* **153** 108828

- [13] Belahmar A, Mikou M, Saidou A M, El Baydaoui R and Bougteb M 2018 *Radiat. Phys. Chem.* **152** 6–11
- [14] Gallo S et al 2017 *Radiat. Environ. Bioph.* **56** 471–80
- [15] Gallo S, Collura G, Iacoviello G, Longo A, Tranchina L, Bartolotta A, Errico F and Marrale M 2017 *Nucl. Instrum. Methods Phys. Res. B* **407** 110–7
- [16] Rushdi M A H and Beshir W B 2019 *Radiat. Phys. Chem.* **162** 121–4
- [17] Waldeland E, Helt-Hansen J and Malinen E 2011 *Radiat. Meas.* **46** 213–8
- [18] www.harwell-dosimeters.co.uk
- [19] Galindo S and Klapp J 2005 *Rev. Mex. Fis.* **51** 193–8
- [20] Ureña-Núñez F, Galindo S and Azorín J 1998 *Appl. Radiat. Isot.* **49** 1657–64
- [21] Ureña-Núñez F, Galindo S and Azorín J 1999 *Appl. Radiat. Isot.* **50** 763–7
- [22] Malinen E, Waldeland E, Hole E O and Sagstuen E 2006 *Spectrochim. Acta A* **63** 861–9
- [23] Belahmar A, Mikou M and El Ghalmi M 2018 *Nucl. Instrum. Methods Phys. Res. B* **431** 19–24
- [24] Waldeland E, Hörling M, Hole E O, Sagstuen E and Malinen E 2010 *Phys. Med. Biol.* **55** 2307–16
- [25] Gabbard F, Davis R H and Bonner T W 1959 *Phys. Rev.* **114** 201
- [26] Lund E, Gustafsson H, Danilczuk M, Sastry M D and Lund A 2004 *Spectrochim. Acta A* **60** 1319–26
- [27] Bortolussi S et al 2018 *Nucl. Instrum. Methods Phys. Res. B* **414** 113–20
- [28] Marrale M, Schmitz T, Gallo S, Hampel G, Longo A, Panzeca S and Tranchina L 2015 *Appl. Radiat. Isot.* **106** 116–20
- [29] Schmitz T et al 2015 *Med. Phys.* **42** 400–11
- [30] Sharpe P H G and Septhon J P 1999 Alanine dosimetry at NPL—the development of a mailed reference dosimetry service at radiotherapy dose levels *Technical Report IAEA-SM-356/65* (National Physical Laboratory, UK)
- [31] X-5 Montecarlo Team 2003 *MCNP: a General Montecarlo n-Particle Transport code (version 5, LA-UR-03-1987)* (Los Alamos, NM: Los Alamos National Laboratory)
- [32] ICRU Report 44 1989 *Tissue Substitutes in Radiation Dosimetry and Measurement* (Bethesda, MD: International Commission on Radiation Units and Measurements)
- [33] Velbeck K J, Luo L Z, Ramlo M J and Rotunda J E 2006 *Radiat. Prot. Dosim.* **119** 255–58
- [34] Ovenall D W and Whiffen D H 1961 *Mol. Phys.* **4** 135–44
- [35] Vestad T A, Gustafsson H, Lund A, Hole E O and Sagstuen E 2004 *Phys. Chem. Chem. Phys.* **6** 3017–22